

Performance test of tree segmentation algorithms for WLS point clouds

R. Bülbül¹, S. Reder¹, J.-P. Mund¹

¹University for Sustainable Development, Schicklerstr. 5 16225 Eberswalde (Germany)
Email: {ramazan.buelbuel; stefan.reder; jan-peter.mund}@hnee.de

1. Introduction

Individual tree detection and delineation of trees in dense laser point clouds provides significant information and tree parameters such as location of the stems, density and as species classification (Ke & Quackenbush, 2011). Wearable Laser Scanner (WLS) makes the point cloud acquisition viable and efficient with the help of the inertial measurement units (IMU). WLS results provide point cloud accuracy at a centimetre level. Further, it simplifies the preparation processes and decreases the processing time compared to stationary terrestrial laser scanner (Cabo C, 2018). Especially, the development of the simultaneous localization and mapping (SLAM) technology and the robotic operative system (ROS) allows to on-the-fly registration of point clouds and trajectories and the processing of 3D map without external positioning systems (Cabo C, 2018).

In this study, we compared three raster-based and two point-cloud-based algorithms, that were developed for the segmentation of LiDAR point clouds with the aim of individual trees detection and segmentation in data products captured with a WLS using SLAM technology.

2. Data and Methods

2.1 Equipment for Scanning

In this research, we've applied a GeoSLAM Zeb Horizon. This WLS scanner provides flexibility in field scans with its 100m range, lightweight, and user-friendly design (Solutions: ZEB Horizon, 2021).

2.2 Study Areas and data acquisition

We scanned 10 small scale plots (30m x 30m) in the arboretum near the forest campus of Eberswalde University which allowed collecting samples of different forest types and tree densities with different tree species and mixtures.

Table 1. Investigation Plots and Ground Truth Data

Plot	Tree Species	Latitude (N)	Longitude (E)	Trees per plot	Trees per ha
1 st Plot	<i>Pseudotsuga menziesii</i> , <i>Fagus sylvatica</i>	52.825672	13.812616	34	378
2 nd Plot	<i>Pinus sylvestris</i> , <i>Fagus sylvatica</i>	52.823815	13.812666	36	400
3 rd Plot	<i>Thuja plicata</i> , <i>Quercus petraea</i> , <i>Fagus sylvatica</i>	52.820535	13.810163	49	544
4 th Plot	<i>Picea abies</i>	52.819896	13.810939	45	500
5 th Plot	<i>Pinus sylvestris</i>	52.819757	13.808905	78	867
6 th Plot	<i>Betula pendula</i>	52.819337	13.809003	40	444
7 th Plot	<i>Larix decidua</i>	52.818644	13.808513	60	667
8 th Plot	<i>Pinus sylvestris</i> , mature stand	52.819285	13.806982	61	678
9 th Plot	<i>Pinus sylvestris</i> , <i>Pseudotsuga menziesii</i> , <i>Quercus petraea</i> , <i>Fagus sylvatica</i>	52.824366	13.802977	38	422
10 th Plot	<i>Pinus sylvestris</i> , pole stand	52.823008	13.799991	123	1367

2.3 Data pre-processing and preparation

Discrete Laser point data from the WLS scanner was processed to a point cloud using the GEOSlam HUB and afterwards clipped to the sample size of 30m x 30m. All point clouds of sample plots were classified into ground and off-ground points by applying the Progressive Morphological Filter (PMF) method (Zhang, et al., 2003). We generated a Digital Terrain Model (DTM) from ground points previously classified using the Inverse Distance Weighting (IDW) interpolation algorithm. Then, we normalized the DTM to generate the terrain normalization according (Liu, Skidmore, Heurich, & Wang, 2017). After terrain normalization, we separated only non-ground points for the further processing and individual tree segmentation.

2.4 Tree segmentation methods applied

After pre-processing and preparation of each point cloud data set mentioned above, we applied several algorithms for individual tree object segmentation algorithms and compared the number of detected trees. The different tree segmentation algorithms are briefly described in the following:

Watershed segmentation (WSS) (Canopy Maxima Model): First, the complement of the canopy maxima model is generated. This model is presumed to be immersed in the water basin. Dividing lines are established to prevent the water from going to both trees and to make the distinction for separating two neighbouring trees and used to identify each individual tree (Chen, 2006).

Particle swarming optimization (PSO) (Franceschi, 2018): Each particle of the swarm moves to a better position in the model towards its own previous local best, and towards the global best after iteration. A fitness function optimized the process. For all particles, a fitness value is calculated each time the extraction algorithm is running, and result will influence the direction of movement of particles through the rest of the in the following iteration (Franceschi, 2018).

Tree centric approach (TCA) (Dalponte 2016) is a raster-based segmentation using local maxima (treetops) to grow individual crowns within a rasterized canopy height model. Initially, to smooth the surface of rasterized CHM and decrease the amount of the local maxima points, a low-pass filter is applied. A local maximum is detected when a pixel has values greater than others in a circular moving window with a size of 5m. The extracted (identified and first return) four neighbouring pixels from CHM after identification and selection of the first return are added to this region if their vertical distance from the local maximum is within the limitation of user defined threshold. These iterations last for every pixel added and finally, a 2D convex hull is applied to the first returns. The ultimate polygons represent the individual segmented trees in the point cloud (Dalponte & Coomes, 2016).

In contrast to the algorithms introduced previously, the **region growth algorithm (RGA)** proposed by Li (2012) work on the point cloud base. The general rationale for this segmentation is that the horizontal gaps between trees are larger at the top than at the bottom. For this reason, segmentation starts by finding the global maximum as seed points for the region growth algorithm and processes discrete points bottom wards. Points are assigned to the nearest treetop, unless the distance is beyond a certain threshold (Li, Guo, Jakubowski, & Kelly, 2012).

The **Adaptive Mean Shift 3D Segmentation (AMS3D)** (Ferraz, 2016) has a similar scope and approach and generates 3D clusters of the individual tree crowns. It starts by calculating local maxima in density and height by using 3D kernels for each point that moves iteratively to denser regions until the kernels converge. Then, 3D clusters are computed by collecting the points that are converged to the same crown. This non-parametric approach is only depending on the size of the kernels, which are adapting to the size of the dense regions using allometric functions (Ferraz, 2016).

2.4 Evaluation

The numbers of trees detected with each segmentation algorithms were compared to the ground-truths data of each plot collected empirically using conventional forestry measures. Finally, we applied a regression analysis to compare the number of detected trees and determine whether the detection rate is changing according to the tree density and if so, to what extent.

3. Results & Discussion

In general, it can be observed that point cloud based approaches (ASM3D, RGA) outperform the raster-based algorithms (WSS, TCA, PSO) (Figure 1) and with a higher tree density, the share of not detected trees is rising (Figure 2).

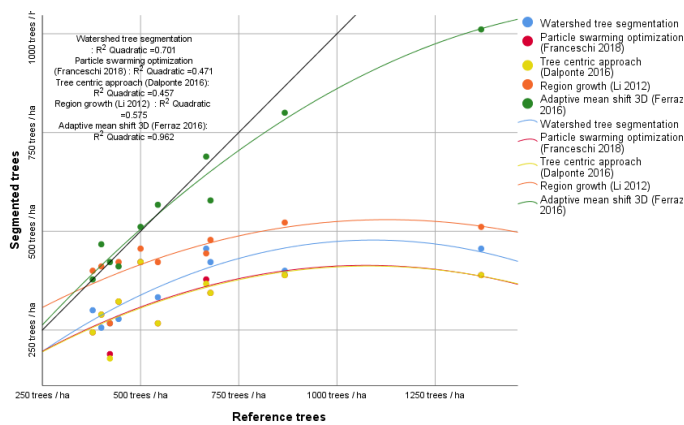


Figure 1 Number of segmented trees detected with different algorithms depending on the tree density of the stands.

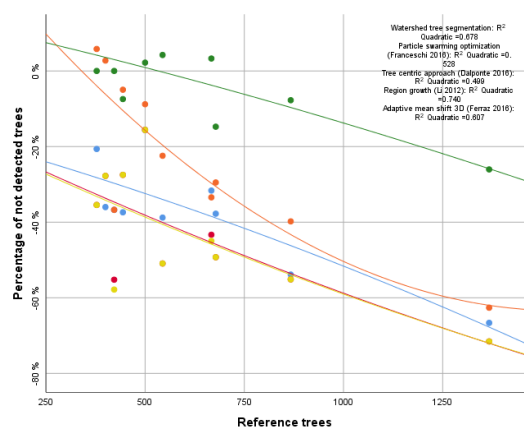


Figure 2 Relation between number of stems and the share of not detected trees.

The ASM3D performed best and, in contrast to other algorithms and more robust to higher tree densities of stands. Even in a pole stand with 1250 trees/ha, only 25% of the trees were not detected, while other approaches missed out more than 60% of the trees. For mature stands with less than 500 trees/ha, more than 90% of the trees were detected, but certain number of crowns were segmented in several parts, resulting in overestimation of the number of trees (Figure 2).

The RGA shows performance comparable to the AMS3D for stands with a density lower than 500 trees/ha. But with higher densities, the performance drops rapidly to detection rates similar of raster-based approaches (Figure 2). As RGA starts from treetops, it is also weak in detection understanding trees and instable processing separation of crowns that are intertwined with each other.

From the raster-based approaches, the WSA showed slightly better performance than the TCA and the PSO, which performed nearly identical. Even in mature stands with densities of less than 500 trees/ha, all raster-based approaches missed out more than 20% of the trees and the detection rates are linear declining with a rising density.

4. Conclusions

In our study, we could show the limits of raster-based segmentation approaches for WLS point clouds, especially in stands with high density. The same shortcomings were observed for the point-cloud-based region growth algorithm which is mainly depended on visible treetops. The ASM3D, developed for LiDAR point clouds, showed the best performance and was able to detect most trees (>85%) up to 850 trees/ha and is only falling off slightly afterwards (1250 trees/ha; 75% detection rate).

Acknowledgements

This proof-of-concept study was conducted as part of the WINMOL-Project (<https://winmol.thuenen.de/>) funded by the Fachagentur Nachwachsende Rohstoffe (FNR) and the Federal Ministry of Food and Agriculture, Germany (BMEL) (FNR funding number: **2220NR024A**)

References

Cabo C, D. P.-G.-A. (2018). Comparing Terrestrial Laser Scanning (TLS) and Wearable Laser Scanning (WLS) for Individual Tree Modeling at Plot Level. *Remote Sensing*, 10(4), 540. doi:doi.org/10.3390/rs10040540

- Chen, Q. B. (2006). Isolating Individual Trees in a Savanna Woodland Using Small Footprint Lidar Data . *Photogrammetric Engineering & Remote Sensing*, 72(8), 923–932. doi:10.14358/pers.72.8.923
- Dalponte, M., & Coomes, D. (2016). Tree-centric mapping of forest carbon density from airborne laser scanning and hyperspectral data. *Methods in Ecology and Evolution*, 7(10), 1236–1245. doi:10.1111/2041-210X.12575
- Ferraz, A. S. (2016). Lidar detection of individual tree size in tropical forests. *Remote Sensing of Environment*, 183, 318–333. doi:10.1016/j.rse.2016.05.028
- Franceschi, S. A. (2018). Identifying treetops from aerial laser scanning data with particle swarming optimization. *European Journal of Remote Sensing*, 51(1), 945–964. doi:10.1080/22797254
- Ke, Y., & Quackenbush, L. J. (2011). A review of methods for automatic individual tree-crown detection and delineation from passive remote sensing. *International Journal of Remote Sensing*, 32(17), 4725–4747. doi:10.1080/01431161.2010.494184
- Li, W., Guo, Q., Jakubowski, M., & Kelly, M. (2012). A New Method for Segmenting Individual Trees from the Lidar Point Cloud. *PHOTOGRAMMETRIC ENGINEERING & REMOTE SENSING*, 78(1), 75–84. doi:10.14358/PERS.78.1.75
- Liu, J., Skidmore, A., Heurich, M., & Wang, T. (2017). Significant effect of topographic normalization of airborne LiDAR data on the retrieval of plant area index profile in mountainous forests. *ISPRS Journal of Photogrammetry and Remote Sensing* *ISPRS Journal of Photogrammetry and Remote Sensing*, 132, 77–87. doi:10.1016/j.isprsjprs.2017.08.005
- Solutions: ZEB Horizon*. (15. February 2021). Von GeoSLAM: <https://geoslam.com/solutions/zeb-horizon/> abgerufen
- Zhang, K., Chen, S.-C., Whitman, D., Shyu, M.-L., Yan, J., & Zhang, C. (2003). A Progressive Morphological Filter for Removing Nonground Measurements From Airborne LIDAR Data. *IEEE TRANSACTIONS ON GEOSCIENCE AND REMOTE SENSING*, 41, 872 - 882. doi:10.1109/TGRS.2003.810682